



ConvFormer: Closing the Gap Between CNN and Vision Transformers

Zimian Wei, Hengyue Pan, Xin Niu, Dongsheng Li

College of Computer, National University of Defense Technology, Changsha 410073, China

E-mail: {weizimian16, hengyuepan, niuxin, dsli}@nudt.edu.cn

Abstract: Vision transformers have shown excellent performance in computer vision tasks. However, the computation cost of their (local) self-attention mechanism is expensive. Comparatively, CNN is more efficient with built-in inductive bias. Recent works show that CNN is promising to compete with vision transformers by learning their architecture design and training protocols. Nevertheless, existing methods either ignore multi-level features or lack dynamic prosperity, leading to sub-optimal performance. In this paper, we propose a novel attention mechanism named MCA, which captures different patterns of input images by multiple kernel sizes and enables input-adaptive weights with a gating mechanism. Based on MCA, we present a neural network named ConvFormer. ConvFormer adopts the general architecture of vision transformers, while replacing the (local) self-attention mechanism with our proposed MCA. Extensive experimental results demonstrated that ConvFormer achieves state-of-the-art performance on ImageNet classification, which outperforms similar-sized vision transformers (ViTs) and convolutional neural networks (CNNs). Moreover, for object detection on COCO and semantic segmentation tasks on ADE20K, ConvFormer also shows excellent performance compared with recently advanced methods. Code and models will be available.

Key words: vision transformer; CNN; attention mechanism; multi-level feature

<https://doi.org/>

CLC number: TP391.4

1 Introduction

Convolution neural networks (CNN) have long been the de-facto feature extractor in the computer vision field. There are several notable properties in CNNs, e.g., translation equivalence and sliding-window manner, making them efficient and suitable for both high-performance GPUs and edge devices. Over the past several years, many efforts have been made to optimize CNN architectures, evolving from manually designed (He et al., 2016a; Simonyan and Zisserman, 2015; Xie et al., 2017; Li et al., 2021) to automatically searched (Liu et al., 2018; Cai et al., 2018, 2019; Howard et al., 2019; Wu et al., 2019; Real et al., 2019; Radosavovic et al., 2020) methods. Excellent works include ResNet (He et al., 2016a), Mo-

bileNet3 (Howard et al., 2019), RegNet (Radosavovic et al., 2020), EfficientNet (Tan and Le, 2019a), and etc. The development of CNN has brought significant improvements in a wide range of visual tasks.

Recently, the newly emerged vision transformers have challenged the dominance of CNN with powerful performance and nice scalability, altering the landscape of network architecture design. As a pioneer work, Dosovitskiy et al. (2020) first introduced ViT from natural language processing (NLP) to the computer vision field, achieving competitive accuracy on ImageNet (Deng et al., 2009). Nevertheless, the computation cost of the global attention mechanism is quadratic according to the image size, which makes vanilla ViT unaffordable for high-resolution downstream tasks, e.g., objective detection and semantic segmentation. To tackle this problem, Swin (Liu et al., 2021b) proposed a local attention trans-

former with a hierarchical design and sliding window strategy, presenting a generic backbone for various visual tasks.

Generally, both CNN and ViT have their pros and cons. With built-in inductive biases, CNNs are more efficient, and capable of modeling local relations. Meanwhile, CNN is easy to train with quick convergence. However, most of them apply static weights, which limits their representation capacity and generality (Dai et al., 2017; Han et al., 2021c). Differently, (local) self-attention in ViT provides data specificity, in which weights are dynamic and predicted from each instance, leading to powerful performance and robustness in large data regimes (Park and Kim, 2022). Unfortunately, the implementation of cross-window self-attention (Liu et al., 2021b; Vaswani et al., 2021; Yang et al., 2021; Huang et al., 2021) is sophisticated and expensive.

To this end, there is a trend to take the merits of both CNNs and ViTs by migrating desired properties of ViTs to CNNs, including the general architecture design, long-range dependency, and data specificity provided by the attention mechanism. ConvNext built a pure CNN family based on ResNet (He et al., 2016a), which performs on par or slightly better than ViT by learning their training procedure and macro/micro-level architecture designs. RepLKNet (Ding et al., 2022) follows the large kernel design in ViT and proposes to learn long-range relations by adopting as large as 31×31 kernel size to enlarge effective receptive fields. Although encouraging performance has been achieved by the above methods, their computation costs are relatively large. Han et al. (2021b) competes favorably with Swin transformer (Liu et al., 2021b) by replacing the local self-attention layer with the dynamic depth-wise convolution layer, while keeping the overall structure unchanged. However, the simple dynamic mechanism design and lack of multi-level features limit its capacity to achieve better performance.

In this paper, we adopt the general architecture of ViT and propose a novel dynamic attention mechanism called MCA. MCA combines small and large kernel sizes for different resolution patterns, which is proved to improve accuracy and efficiency in (Tan and Le, 2019b). Meanwhile, it provides data adaptability by a lightweight gating mechanism, with which the channel-wise relationships are captured and the representational power of the net-

work is enhanced. Based on the MCA, we present a novel CNN called ConvFormer. ConvFormer can be applied as a general vision backbone for different tasks. Extensive experimental results demonstrate that ConvFormer shows state-of-the-art performance and closes the gap between vision transformers and CNNs. Generally, the contributions of this paper are three folds:

- We propose a novel attention mechanism MCA, which is dynamic and adopts multiple convolution kernel sizes for different resolution patterns.
- Based on MCA, we design a general CNN backbone named ConvFormer, which combines the advantages of ViT and CNN.
- We conduct extensive experiments on multiple vision tasks including image classification, object detection, and semantic segmentation to evaluate ConvFormer. The experimental results demonstrated that ConvFormer achieves state-of-the-art performance.

2 Related works

Vision Transformers The transformers are initially introduced in (Vaswani et al., 2017) and have spread widely in the field of Natural Language Processing. Dosovitskiy et al. (2020) first adapts transformer in computer vision, in which images are split up as a series of patches and transformed into vectors to produce input tokens. The global self-attention module in vanilla vision transformer (Dosovitskiy et al., 2020; Touvron et al., 2021b) measures the relationships between pairs of input tokens, leading to quadratic computation costs with regard to the number of input tokens. Recent advancements (Liu et al., 2021b; Vaswani et al., 2021; Yang et al., 2021) modified the global self-attention to local self-attention, which performs self-attention within non-overlapped local windows and adopts a hierarchical design to improve efficiency. Still, the cross-window connection like expanding (Yang et al., 2021), shifting (Liu et al., 2021b), or shuffling (Huang et al., 2021) is required to expand the receptive field of local self-attention, which is sophisticated and unnecessary. In this paper, we replace the (local) self-attention layer with our proposed MCA to compete favorably with the previous Transformer-based models.

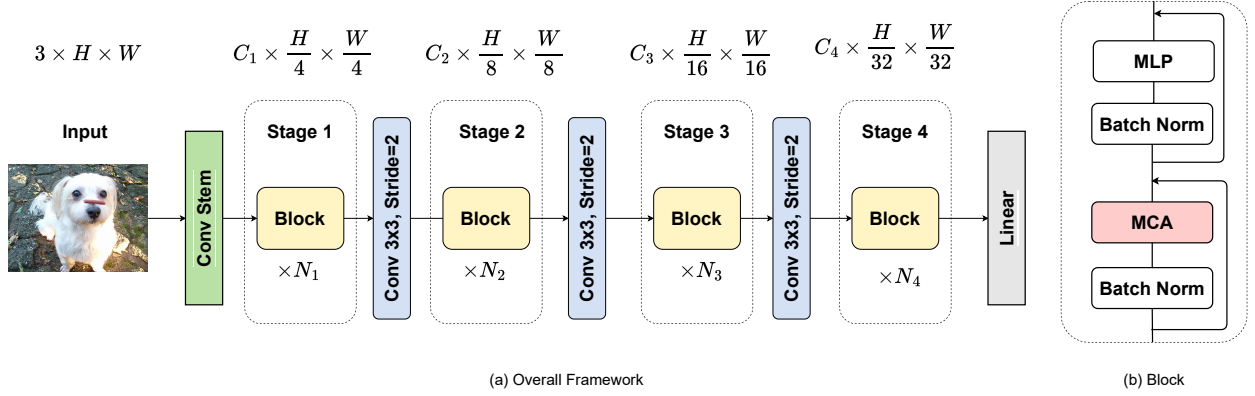


Fig. 1 (a) The overall framework of ConvFormer. Following (Yu et al., 2021; Liu et al., 2021b), ConvFormer adopts the hierarchical architecture with 4 stages, and each stage consists of multiple blocks. C_i, N_i refer to the feature dimension and block number in stage i , respectively. (b) The basic block in ConvFormer. We apply the modular design in vision transformers, while replacing the (local) self-attention layer with MCA.

Attention Mechanism Motivated by the human visual system that pays attention to salient regions of images, attention mechanisms can be coarsely interpreted as a dynamic importance weight of input features. According to (Guo et al., 2021), attention mechanisms can be divided into four basic categories: channel attention (Hu et al., 2018b; Gao et al., 2019; Lee et al., 2019), temporal attention (Li et al., 2019a; Liu et al., 2021d), branch attention (Li et al., 2019b; Yang et al., 2019) and spatial attention (Wang et al., 2018; Hu et al., 2018a; Zhao et al., 2018; Dosovitskiy et al., 2020). Channel attention adaptively recalibrates the weight of each channel to pay attention to different objects; temporal attention emphasizes capturing the interaction between frames and determining when to pay attention; branch attention is a dynamic branch selection mechanism that enables information flows from different branches; spatial attention generates attention masks to adaptively select important spatial regions. In this paper, the channel attention mechanism is applied in MCA to capture channel-wise relationships, while multi-level feature learning is adopted to improve representation ability.

3 Approaches

In this section, we first present details of MCA. Then we show the general structure in the basic block of ConvFormer and present different architecture designs in our ConvFormer family.

3.1 MCA

We illustrate the structure of MCA in Figure 2. The two key components in MCA are the multi-level feature fusion and gating mechanism. Multi-level feature fusion is able to capture different patterns with various resolutions of input images, combining multi-scale feature maps. Meanwhile, the gating mechanism is introduced to perform feature recalibration, which learns to selectively emphasize informative features and suppress nontrivial ones.

Assuming that the input of MCA is X . As depicted in Figure 2, a 1×1 convolution layer is applied to expand the number of channels by N times. Then, a parallel design of 3×3 , 5×5 , 7×7 depth-wise convolution is introduced to learn multi-scale features. BatchNorm and ReLU are followed to prevent overfit when training. Next, in order to apply a residual connection for better optimization, we apply a 1×1 convolution layer to reduce the number of channels as the original input X . The above operators can be expressed as

$$\begin{aligned} X_E &= \text{Conv}_{\text{expand}} 1 \times 1(X), \\ X_1, X_2, X_3 &= \text{Parallel}_{3 \times 3, 5 \times 5, 7 \times 7}(X_E), \\ X_P &= \text{ReLU}(\text{BN}(X_1 + X_2 + X_3)), \\ X' &= X + \text{Conv}_{1 \times 1}(X_P), \end{aligned} \quad (1)$$

where $\text{Parallel}_{3 \times 3, 5 \times 5, 7 \times 7}$ contains multi-branch of 3×3 , 5×5 , 7×7 convolution layers. Following (Ding et al., 2022; Guo et al., 2022), we apply dilated depth-wise convolution with kernel size 5×5 , 7×7 , dilate rate as 2, 3 to obtain larger receptive field.

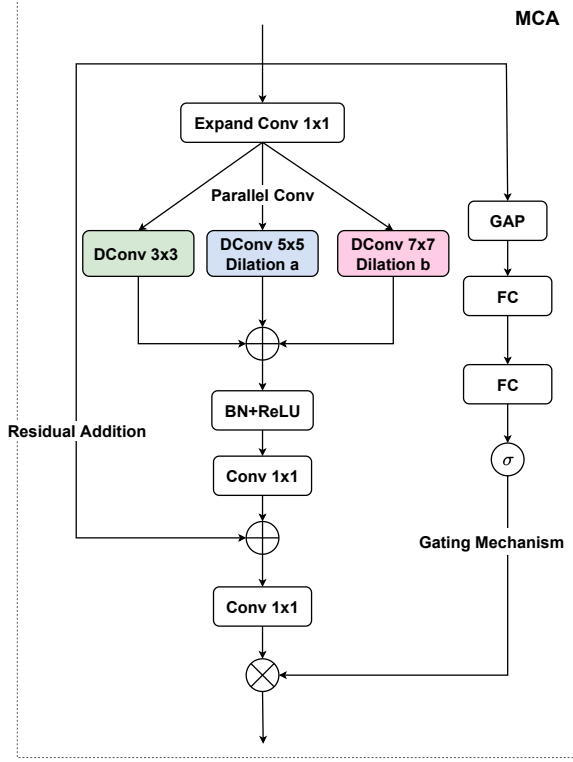


Fig. 2 The framework of MCA. The design of MCA is originated from (Wu et al., 2021). Differently, we improve it with multi-level resolution patterns by applying different kernel sizes. DConv, GAP, and FC refer to depth-wise convolution, global average pool, and fully connected layer, respectively. σ refers to sigmoid function.

For the gating mechanism, we apply a global average pooling (GAP) layer to obtain global information, followed by two successive fully connected layers. At last, a sigmoid function is applied to compute the attention vector. The operations in the gating mechanism can be formulated as follows:

$$\begin{aligned} V &= \text{ReLU}(\text{FC}(\text{GAP}(X))), \\ \text{Attn} &= \text{Sigmoid}(\text{FC}(V)), \end{aligned} \quad (2)$$

To re-calibrate the fused feature by the gating mechanism, we have:

$$\text{Output} = \text{Attn} \otimes \text{Conv}1 \times 1(X'), \quad (3)$$

With the dynamic mechanism and multi-level feature learning in MCA, the model capacity can be largely enhanced.

3.2 ConvFormer

We build ConvFormer with a hierarchical design similar to traditional CNNs (Krizhevsky et al., 2012;

Simonyan and Zisserman, 2015; He et al., 2016a) and recent local vision transformers (Liu et al., 2021b; Wang et al., 2021b). Figure 1 (a) presents the overall framework of ConvFormer and Figure 1 (b) shows the basic block in ConvFormer.

The input I is first processed by the convolution stem module, which consists of a 7×7 convolution layer with a stride of 2, a 3×3 convolution layer with a stride of 1, and a non-overlapping 2×2 convolution layer with a stride of 2. In this way, the input features are generated with a spatial size of $\frac{H}{4} \times \frac{W}{4}$.

$$X = \text{ConvStem}(I), \quad (4)$$

we denote $X \in \mathbb{R}^{N \times C_1 \times \frac{H}{4} \times \frac{W}{4}}$ as input features with batch size N and number of channels C_1 .

Then, the input features are fed to repeated ConvFormer blocks, each of which consists of two sub-blocks. Specifically, the main components of the first sub-block include MCA and the BatchNorm module, which we present as

$$Y = \text{MCA}(\text{BN}(X)) + X, \quad (5)$$

where $\text{BN}(\cdot)$ denotes a Batch Normalization (Ioffe and Szegedy, 2015). $\text{MCA}(\cdot)$ is depicted in Section 3.1.

The second sub-block consists of two fully-connected layers and a non-linear activation GELU (Hendrycks and Gimpel, 2016). The output of the MLP module is formulated as follows:

$$Z = \text{GELU}(W_1(\text{BN}(Y))W_2 + Y, \quad (6)$$

where $W_1 \in \mathbb{R}^{C_i \times rC_i}$ and $W_2 \in \mathbb{R}^{rC_i \times C_i}$ are learnable parameters in fully connected layers. r is the MLP expansion ratio for the number of channels; C_i is the number of channels in the corresponding stage.

Based on the above ConvFormer block, we formulate ConvFormer-S and ConvFormer-L with different model sizes. The numbers of channels responding to the four stages are identical for both ConvFormer-S and ConvFormer-L, which are set as 64, 128, 320, and 512. Differently, ConvFormer-L is larger with respect to block numbers. Specifically, stages 1, 2, 3, and 4 of ConvFormer-S contain 2, 2, 6, 2 blocks, while that for ConvFormer-L are 3, 3, 12, 3, respectively. Their detailed architecture designs are shown in Table 1.

Table 1 The detailed setting for different versions of ConvFormer. ER represents the expansion ratio in the MLP module.

stage	output size	ER	ConvFormer-S	ConvFormer-L
1	$\frac{H}{4} \times \frac{W}{4} \times C$	8	$C = 64$ $L = 2$	$C = 64$ $L = 3$
2	$\frac{H}{8} \times \frac{W}{8} \times C$	8	$C = 128$ $L = 2$	$C = 128$ $L = 3$
3	$\frac{H}{16} \times \frac{W}{16} \times C$	4	$C = 320$ $L = 6$	$C = 320$ $L = 12$
4	$\frac{H}{32} \times \frac{W}{32} \times C$	4	$C = 512$ $L = 2$	$C = 512$ $L = 3$
Parameters (M)			26.7	45.0
FLOPs (G)			5.0	8.7

4 Experiments

We evaluate ConvFormer on three representative vision tasks, including image classification, object detection, and semantic segmentation. Ablation studies and visualizations are also presented to thoroughly study the effectiveness of ConvFormer. All experiments are conducted on 8 NVIDIA A100 GPUs.

4.1 Image classification

We conduct image classification experiments on ImageNet-1K (Deng et al., 2009), which contains 1.28M training images and 50K validation images, covering 1000 different categories. We report Top-1 accuracy, parameters, and FLOPs to compare different models.

4.1.1 Experimental Setup

We follow the main training strategies in PoolFormer (Yu et al., 2021). Specifically, Cutmix (Yun et al., 2019), RandAugment (Cubuk et al., 2020), Mixup (Zhang et al., 2018), and Label Smoothing regularization (Szegedy et al., 2016) are applied to augment the training data. Each model is trained for 300 epochs with AdamW optimizer (Kingma and Ba, 2014; Loshchilov and Hutter, 2018), and a total batch size of 1024 on 8 GPUs. The initial learning rate is set as $1e-3$. We adopt a warm-up strategy and cosine decay schedule (Loshchilov and Hutter, 2016) to adjust the learning rate during training. Stochastic depth (Huang et al., 2016) with degree 0.2 is used to enhance performance. The implementation is based

on the `timm` codebase¹.

4.1.2 Results

Table 2 summarizes the experimental results on ImageNet-1K classification. Despite the simple architecture design, ConvFormer attains consistent improvement over other state-of-the-art models. For example, ConvFormer-S outperform ResMLP-24 (Touvron et al., 2021a) by 3.4% top-1 accuracy, while requiring less parameters (30.0 M \rightarrow 26.7 M) and computation cost (6.0 G \rightarrow 5.0 G FLOPs). When compared with recently well-established ViTs like Swin-S (Liu et al., 2021b) and Focal-S (Yang et al., 2021), ConvFormer also shows better performance. Specifically, Swin-S obtains 83.0% top-1 accuracy with 49.6M parameters and 8.7G FLOPs while ConvFormer-L reaches 83.6% with 9.3% fewer parameters (45M). Besides, Focal-S attains a slightly worse accuracy of 83.5% but requires 14% more parameters. Comparatively, ConvNeXt (Liu et al., 2022) is an outstanding CNN that learns architecture designs and training schedules from ViTs for better performance. ConvFormer-L outperforms ConvNeXt-S by 0.5%, while reducing the model size by 10%. The experiment results demonstrate the superiority of ConvFormer.

4.2 Object detection

In this section, we conduct experiments on COCO 2017, a challenging benchmark for object detection which includes 118K training images and 5K validation images. Average Precision (AP) is reported as model performance. Specifically, AP_{50} , and AP_{75} are the average precision at IOU=0.5 and IOU=0.75, where IoU evaluates the degree of overlap between the ground truth and prediction. AP_S , AP_M , and AP_L are the average precision for small, medium, and large objects. AP^b and AP^m refer to bounding box AP and mask AP.

4.2.1 Experimental Setup

We evaluate ConvFormer on top of two standard detectors, namely RetinaNet (Lin et al., 2017b) and Mask R-CNN (He et al., 2017b). We initialize the backbone with ImageNet pre-trained weights and newly added layers with Xavier (Glorot and Bengio, 2010), respectively. Each model is trained with

¹<https://github.com/rwightman/pytorch-image-models>

Table 2 Compare with the state-of-the-art methods on the ImageNet validation set. Params means parameter. GFLOPs donates floating point operations. Top-1 Acc represents Top-1 accuracy.

Method	Params. (M)	GFLOPs	Top-1 Acc (%)
T2T-ViT _t -14 (Yuan et al., 2021)	21.5	6.1	81.7
PVT-Small (Wang et al., 2021c)	24.5	3.8	79.8
TNT-S (Han et al., 2021a)	23.8	5.2	81.5
gMLP-S (Liu et al., 2021a)	20.0	4.5	79.6
Swin-T (Liu et al., 2021c)	28.3	4.5	81.3
PoolFormer-S24 (Yu et al., 2021)	21.4	3.6	80.3
ResMLP-24 (Touvron et al., 2021a)	30.0	6.0	79.4
Twins-SVT-S (Chu et al., 2021)	24.0	2.8	81.7
GFNet-S (Rao et al., 2021)	25.0	4.5	80.0
PVTv2-B2 (Wang et al., 2021a)	25.4	4.0	82.0
Focal-T (Yang et al., 2021)	29.1	4.9	82.2
ConvNeXt-T (Liu et al., 2022)	28.6	4.5	82.1
ConvFormer-S	26.7	5.0	82.8
PVT-Medium (Wang et al., 2021c)	44.2	6.7	81.2
PVTv2-B3 (Wang et al., 2021a)	45.2	6.9	83.2
Focal-S (Yang et al., 2021)	51.1	9.1	83.5
Swin-S (Liu et al., 2021c)	49.6	8.7	83.0
ConvNeXt-S (Liu et al., 2022)	50.0	8.7	83.1
ConvFormer-L	45.0	8.7	83.6

Table 3 Object detection on COCO 2017 dataset. #P refers to the model parameter. RetinaNet 1× means models are built on RetinaNet (Lin et al., 2017a) and trained for 12 epochs. AP₅₀, AP₇₅ are the average precision at IOU=0.5 and IOU=0.75, and AP_S, AP_M, and AP_L are the average precision for small, medium, and large objects.

Backbone	RetinaNet 1×						
	#P (M)	AP	AP ₅₀	AP ₇₅	AP _S	AP _M	AP _L
ResNet50 (He et al., 2016b)	37.7	36.3	55.3	38.6	19.3	40.0	48.8
PVT-Small (Wang et al., 2021c)	34.2	40.4	61.3	43.0	25.0	42.9	55.7
PoolFormer-S36 (Yu et al., 2021)	40.6	39.5	60.5	41.8	22.5	42.9	52.4
LIT-S (Pan et al., 2022)	39.0	41.6	62.7	44.1	25.6	44.7	56.5
ConvFormer-S	36.4	42.9	63.1	45.8	26.4	46.8	56.3
ResNet101 (He et al., 2016b)	56.7	38.5	57.8	41.2	21.4	42.6	51.1
ResNeXt101-32x4d (Xie et al., 2017)	56.4	39.9	59.6	42.7	22.3	44.2	52.5
PVT-Medium (Wang et al., 2021c)	53.9	41.9	63.1	44.3	25.0	44.9	57.6
ConvFormer-L	54.8	43.1	64.0	46.1	27.2	47.3	58.3

AdamW (Loshchilov and Hutter, 2018) optimizer, a total batch size of 16 on 8 GPUs. The initial learning rate is set as 1×10^{-4} . We adopt 1× training schedule (12 epochs) in PVT (Wang et al., 2021b) and PoolFormer (Yu et al., 2021) to train all detection models. Our implementation is based on the `mmdetection` (Chen et al., 2019) codebase.

4.2.2 Results

Table 3 and Table 4 present experimental results on COCO under RetinaNet 1x (Lin et al., 2017b) and Mask R-CNN 1x (He et al., 2017b) settings, respectively. It can be observed that ConvFormer concisely outperforms previous SOTA methods. When equipped with RetinaNet 1x (Lin et al., 2017b) setting, ConvFormer-S achieves gains

Table 4 Object detection and instance segmentation on COCO 2017 dataset. #P means parameter. Mask R-CNN 1× represents that models are based on Mask R-CNN (He et al., 2017a) and trained for 12 epochs. AP^b and AP^m means bounding box AP and mask AP, respectively.

Backbone	Mask R-CNN 1×						
	#P (M)	AP^b	AP_{50}^b	AP_{75}^b	AP^m	AP_{50}^m	AP_{75}^m
ResNet50 (He et al., 2016b)	44.2	38.0	58.6	41.4	34.4	55.1	36.7
PVT-Small (Wang et al., 2021c)	44.1	40.4	62.9	43.8	37.8	60.1	40.3
PoolFormer-S36 (Yu et al., 2021)	50.5	41.0	63.1	44.8	37.7	60.1	40.0
LIT-S (Pan et al., 2022)	48.0	42.9	65.6	46.9	39.6	62.3	42.4
ConvFormer-S	46.3	43.1	65.7	47.1	39.8	62.8	42.8
ResNet101 (He et al., 2016b)	63.2	40.4	61.1	44.2	36.4	57.7	38.8
ResNeXt101-32x4d (Xie et al., 2017)	62.8	41.9	62.5	45.9	37.5	59.4	40.2
PVT-Medium (Wang et al., 2021c)	63.9	42.0	64.4	45.6	39.0	61.6	42.1
ConvFormer-L	64.7	43.4	66.0	47.7	40.2	63.5	43.7

Table 5 Results of semantic segmentation on ADE20K (Zhou et al., 2019) validation set. The pre-trained ConvFormer-S is plugged in Semantic FPN (Kirillov et al., 2019a) and UperNet (Xiao et al., 2018) frameworks, and training/validation schemes are following (Yu et al., 2021) and (Liu et al., 2021c). Note that the difference in the number of parameters between two ConvFormer-S is due to the usage of semantic FPN and UperNet.

Method	Backbone	#Param (M)	mIoU (%)
Semantic FPN (Kirillov et al., 2019a)	ResNet101 (He et al., 2016b)	47.5	38.8
	ResNeXt101-32x4d (Xie et al., 2017)	47.1	39.7
	PoolFormer-S36 (Yu et al., 2021)	34.6	42.0
	PVT-Medium (Wang et al., 2021c)	48.0	41.6
	TwinP-S (Chu et al., 2021)	28.4	44.3
	VAN-B2 (Guo et al., 2022)	30.0	46.7
	ConvFormer-S	30.4	47.2
UperNet (Xiao et al., 2018)	ConvNeXt-T (Liu et al., 2022)	60.0	46.7
	Swin-T (Liu et al., 2021c)	60.0	46.1
	TwinP-S (Chu et al., 2021)	54.6	46.2
	Focal-T (Yang et al., 2021)	62.0	45.8
	ConvFormer-S	56.6	47.6

of +3.4 AP over PoolFormer-S36 (Yu et al., 2021), while reducing 10% model size. Similar results are observed in Mask R-CNN 1x (He et al., 2017b) settings. For example, ConvFormer-S has fewer parameters compared to LIT-S (Pan et al., 2022) (46.3 M vs. 48.0 M), but surpasses LIT-S by 0.2 bounding box AP and 0.2 mask AP. Overall, ConvFormer achieves excellent performance in recognizing multi-scale visual objects, clearly demonstrating its effectiveness.

4.3 Semantic segmentation

We apply ADE20K (Zhou et al., 2017) to evaluate the models for semantic segmentation. The

ADE20K dataset contains 20K training images and 2K validation images from 150 different semantic categories. mIoU (mean Intersection Over Union) is applied to measure the model performance, which is the class-averaged IoU that quantifies the overlap between the target masks and prediction outputs.

4.3.1 Experimental Setup

We apply Semantic FPN (Kirillov et al., 2019a) and UperNet (Xiao et al., 2018) as main frameworks to evaluate our ConvFormer backbones. Similar to the object detection task, pre-trained weights on ImageNet-1K are utilized to initialize the backbones. Newly added layers are initialized by Xavier (Glo-

Table 6 Ablation study of different modules in MCA. Block numbers are modified to achieve comparable computation complexity. Top-1 accuracy (Acc) on ImageNet validation, Average Precision (AP) on COCO, and mIoU on ADE20K are applied to show the effectiveness of each component. We adopt RetinaNet (Lin et al., 2017b) and Semantic FPN (Kirillov et al., 2019a) as main frameworks, and use ImageNet pre-trained ConvFormer-S variants as backbones for object detection and semantic segmentation, respectively. Parameters and FLOPs are calculated under the ImageNet classification setting.

ConvFormer-Variant	Blocks	Params. (M)	FLOPs(G)	ImageNet Top-1 Acc	COCO AP	ADE20k mIoU
w/o Expand Conv 1x1	2, 2, 12, 2	26.9	5.0	82.8	42.7	46.3
w/o Parallel Conv	2, 2, 6, 2	26.2	4.9	82.5	41.6	46.0
w/o Residual Add	2, 2, 6, 2	26.7	5.0	82.6	42.3	46.5
w/o Gating Mechanism	2, 2, 7, 2	26.2	5.4	82.7	42.4	45.7
ConvFormer-S	2, 2, 6, 2	26.7	5.0	82.8	42.9	47.2

rot and Bengio, 2010). We train each model with AdamW (Loshchilov and Hutter, 2018) optimizer, a total batch size of 16 on 8 GPUs. When equipped with Semantic FPN (Kirillov et al., 2019a), we follow the 40K-iteration training scheme in (Wang et al., 2021b; Yu et al., 2021), *e.g.*, the learning rate is set as 2×10^{-4} and decays by polynomial schedule with a power of 0.9. Comparatively, we adopt the 160K-iteration training scheme in (Liu et al., 2021c) for UperNet. Specifically, the learning rate is set as 6×10^{-5} with 1500 iteration warmup and linear learning rate decay. Our implementation is based on the `mmsegmentation` codebase².

4.3.2 Results

Table 5 lists the ADE20K semantic segmentation performance of different backbones using FPN (Kirillov et al., 2019b) and UperNet (Xiao et al., 2018). Generally, ConvFormer consistently outperforms other SoTA backbones. When using Semantic FPN (Kirillov et al., 2019a) for semantic segmentation, ConvFormer-S surpasses VAN-B2 (Guo et al., 2022) by 0.5 mIoU with similar computation cost. Moreover, although the parameter of ConvFormer-S is 37% smaller than that of PVT-Medium (Wang et al., 2021c), the mIoU is still 5.6 points higher (47.2 vs 41.6). When applying UperNet as the framework, our model outperforms ConvNeXt-T (Liu et al., 2022) by 0.9 mIoU, with about 6% model size reduction. Additionally, ConvFormer-S is 1.8 mIoU higher than Focal-T (Yang et al., 2021) with 9% decreased parameters. These results indicate that ConvFormer backbone

enables powerful features for semantic segmentation, due to the elegant designs.

4.4 Ablation studies

In this section, we conduct ablation studies on each component of MCA module to shed light on various architecture designs. ConvFormer-S is adopted as our baseline model, based on which we develop several variant models. To achieve comparable model complexity, we modify some block numbers. Results on ImageNet-1K (Deng et al., 2009) classification, COCO (Lin et al., 2014a) object detection, and ADE20K (Zhou et al., 2017) semantic segmentation are reported to compare ConvFormer-S and its variants. Details are as follows:

Expand Conv The Expand Conv module expands the number of channels of input features to a higher dimension. We reduce the expand ratio N from 4 to 1, while increasing the block number in the third stage to 12 to achieve coarsely identical model complexity. It can be observed from Table 6 that the Top-1 accuracy on ImageNet-1K is comparable, while the performance of object detection and semantic segmentation is dropped with -0.2 AP on COCO and -0.9 mIoU on ADE20K. This result demonstrated that the expansion ratio in Expand Conv module is favorable to enhance performance for downstream tasks.

Parallel Conv Parallel Conv module applies multi-branch structure with different kernel sizes, aiming to capture different types of patterns from input images. To provide a comparison, we replace the Parallel Conv module with a single 7×7 convo-

²<https://github.com/open-mmlab/msegmentation>

lution layer. Table 6 shows that the Parallel Conv module brings about improvements of +0.3% Top-1 accuracy on ImageNet-1K, +1.3 AP on COCO, and +1.2 mIoU on ADE20K. This phenomenon shows that the Parallel Conv module is superior to a single-branch convolution layer on three visual tasks with minor computation increases.

Residual Addition Residual Addition is helpful for gradient propagating across multiplier layers. We remove the Residual Addition module to test its effect on ConvFormer-S. As presented in Table 6, performance drops (-0.2% Top-1 accuracy on ImageNet-1K, -0.6 AP on COCO, and -0.7 mIoU on ADE20K) are observed for ConvFormer-S without Residual Addition module. Therefore, we keep the Residual Addition module by default.

Gating Mechanism The gating mechanism is introduced in ConvFormer for the data-adaptive property. Specifically, it produces a collection of per-channel modulation weights, which introduces promising improvements to the representative learning capacity of deep networks. Profited from it, ConvFormer-S achieves improvements of +0.1% Top-1 accuracy on ImageNet-1K, +0.5 AP on COCO, and +1.5 mIoU on ADE20K. The above results indicate the essential of the gating mechanism.

4.5 Visualization

In this section, we show Grad-CAM (Selvaraju et al., 2017) on ImageNet classification and visualize results on downstream visual tasks to better analyze ConvFormer.

Grad-CAM We utilize Grad-CAM to localize discriminative regions generated by Swin-T (Liu et al., 2021c), ResNet50 (He et al., 2016a) and ConvFormer-S in image classification task. Lighter colors in Grad-CAM results refer to stronger attention regions. It can be observed from Fig. 3 that the highlighted class activation area of ConvFormer-S is more accurate. The visualizations clearly demonstrate the effectiveness of our method.

Object Detection and Semantic Segmentation

In Fig. 4, we present some qualitative object detection on COCO val2017 (Lin et al., 2014b), and semantic segmentation results on ADE20K (Zhou

et al., 2017). Specifically, ImageNet pre-trained ConvFormer-S is plugged in dense prediction models, *i.e.*, RetinaNet (Lin et al., 2017a) for object detection, and UperNet (Xiao et al., 2018) for semantic segmentation. The results indicate that ConvFormer can be applied as a general backbone for downstream tasks, and obtain strong results.

5 Conclusions and Future Work

In this paper, we have introduced ConvFormer, a novel efficient vision backbone that outperforms most similar-sized state-of-the-art models on ImageNet and downstream tasks. We have also presented MCA, the key component of ConvFormer which shows much efficiency over the existing (local) self-attention mechanisms. Future work may include adapting ConvFormer to other tasks such as video processing and multi-modal recognition, or extending MCA to a hybrid design with existing excellent CNN or self-attention mechanisms to further enhance performance.

References

- Cai H, Zhu L, Han S, 2018. Proxylessnas: Direct neural architecture search on target task and hardware. *arXiv preprint arXiv:1812.00332*, .
- Cai H, Gan C, Wang T, et al., 2019. Once-for-all: Train one network and specialize it for efficient deployment. *arXiv preprint arXiv:1908.09791*, .
- Chen K, Wang J, Pang J, et al., 2019. MMDetection: Open mmlab detection toolbox and benchmark. *arXiv preprint arXiv:1906.07155*, .
- Chu X, Tian Z, Wang Y, et al., 2021. Twins: Revisiting the design of spatial attention in vision transformers. *NeurIPS*, 34.
- Cubuk ED, Zoph B, Shlens J, et al., 2020. RandAugment: Practical automated data augmentation with a reduced search space. *Proceedings of the IEEE/CVF Conference on Computer Vision and Pattern Recognition Workshops*, p.702-703.
- Dai J, Qi H, Xiong Y, et al., 2017. Deformable convolutional networks. *ICCV*, p.764-773.
- Deng J, Dong W, Socher R, et al., 2009. Imagenet: A large-scale hierarchical image database. *2009 IEEE conference on computer vision and pattern recognition*, p.248-255.
- Ding X, Zhang X, Han J, et al., 2022. Scaling up your kernels to 31x31: Revisiting large kernel design in cnns. *Proceedings of the IEEE/CVF Conference on Computer Vision and Pattern Recognition*, p.11963-11975.
- Dosovitskiy A, Beyer L, Kolesnikov A, et al., 2020. An image is worth 16x16 words: Transformers for image recognition at scale. *International Conference on Learning Representations*.

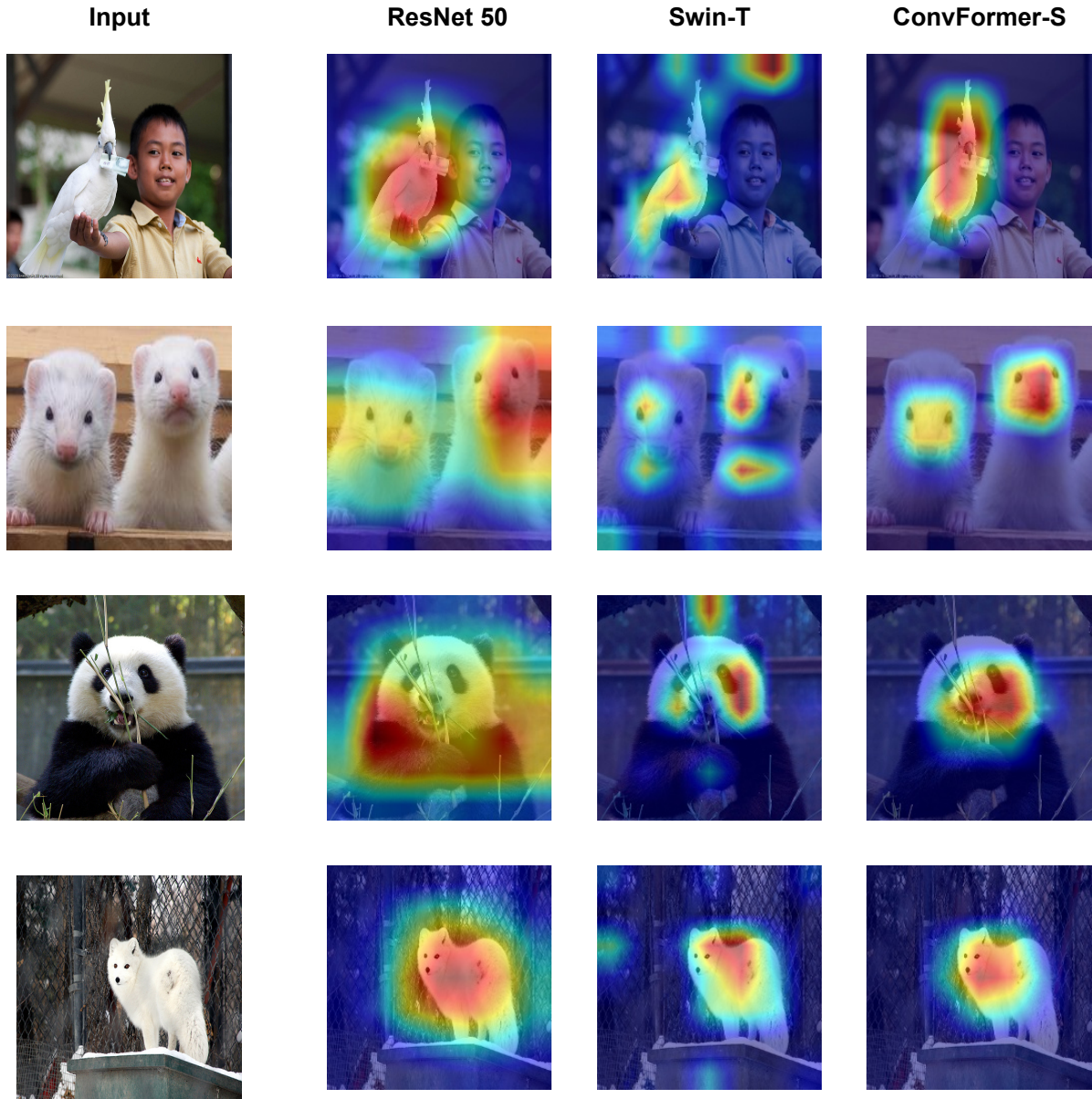


Fig. 3 Visualization results produced by using Grad-CAM (Selvaraju et al., 2017) on images selected from the ImageNet validation dataset. We compare different CAMs generated by Swin-T (Liu et al., 2021c), ResNet50 (He et al., 2016a) and ConvFormer-S.

Gao Z, Xie J, Wang Q, et al., 2019. Global second-order pooling convolutional networks. Proceedings of the IEEE/CVF Conference on Computer Vision and Pattern Recognition, p.3024-3033.

Glorot X, Bengio Y, 2010. Understanding the difficulty of training deep feedforward neural networks. Proceedings of the thirteenth international conference on artificial intelligence and statistics, p.249-256.

Guo MH, Xu TX, Liu JJ, et al., 2021. Attention mechanisms in computer vision: A survey. *arXiv preprint arXiv:211107624*, .

Guo MH, Lu CZ, Liu ZN, et al., 2022. Visual attention network. *arXiv preprint arXiv:220209741*, .

Han K, Xiao A, Wu E, et al., 2021a. Transformer in transformer. *arXiv preprint arXiv:210300112*, .

Han Q, Fan Z, Dai Q, et al., 2021b. On the connection between local attention and dynamic depth-wise convolution. International Conference on Learning Representations.

Han Y, Huang G, Song S, et al., 2021c. Dynamic neural networks: A survey. *IEEE Transactions on Pattern Analysis and Machine Intelligence*, .

He K, Zhang X, Ren S, et al., 2016a. Deep residual learning for image recognition. Proceedings of the IEEE conference on computer vision and pattern recognition, p.770-778.

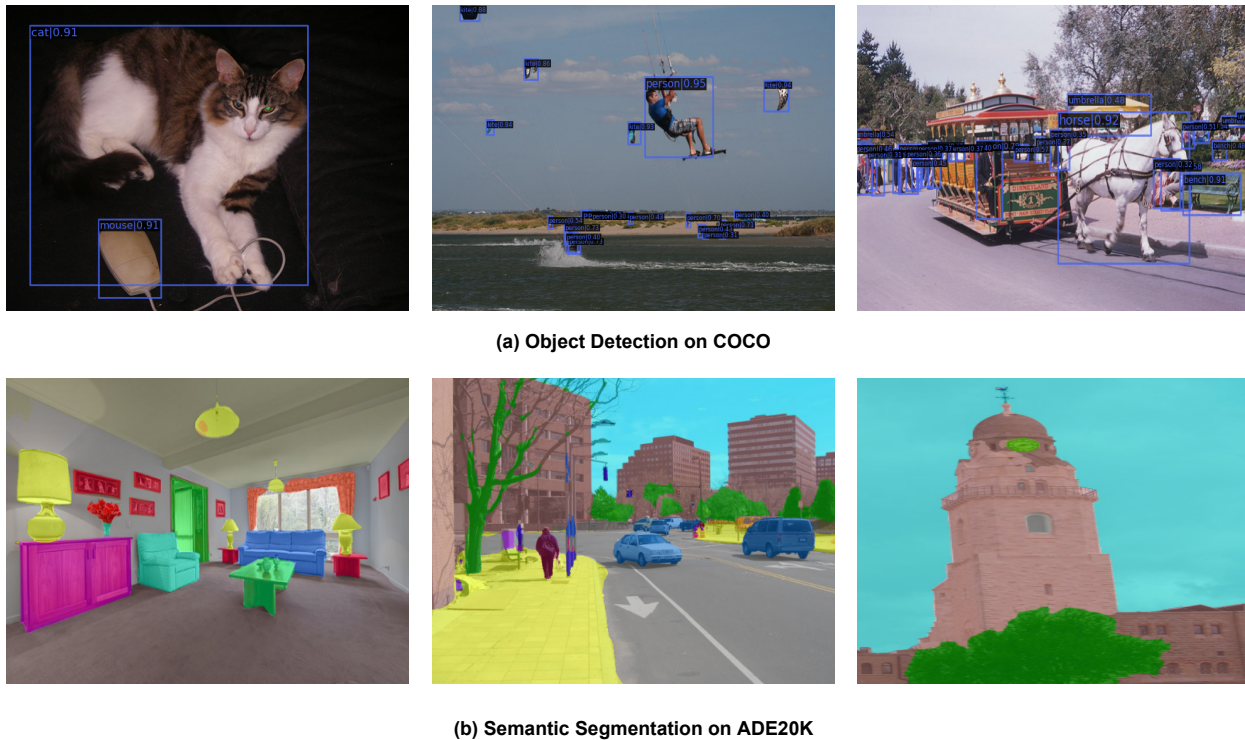


Fig. 4 Visualization results of object detection on COCO val2017 (Lin et al., 2014b), and semantic segmentation on ADE20K (Zhou et al., 2017). We apply pre-trained ConvFormer-S as the backbone, while adopting RetinaNet (Lin et al., 2017a) and UperNet (Xiao et al., 2018) as frameworks to generate results for object detection and semantic segmentation, respectively.

- He K, Zhang X, Ren S, et al., 2016b. Deep residual learning for image recognition. CVPR, p.770-778.
- He K, Gkioxari G, Dollár P, et al., 2017a. Mask r-cnn. ICCV.
- He K, Gkioxari G, Dollár P, et al., 2017b. Mask r-cnn. Proceedings of the IEEE international conference on computer vision, p.2961-2969.
- Hendrycks D, Gimpel K, 2016. Gaussian error linear units (gelus). *arXiv preprint arXiv:160608415*, .
- Howard A, Sandler M, Chu G, et al., 2019. Searching for mobilenetv3. Proceedings of the IEEE/CVF international conference on computer vision, p.1314-1324.
- Hu J, Shen L, Albanie S, et al., 2018a. Gather-excite: Exploiting feature context in convolutional neural networks. *NeurIPS*, 31.
- Hu J, Shen L, Sun G, 2018b. Squeeze-and-excitation networks. CVPR, p.7132-7141.
- Huang G, Sun Y, Liu Z, et al., 2016. Deep networks with stochastic depth. European conference on computer vision, p.646-661.
- Huang Z, Ben Y, Luo G, et al., 2021. Shuffle transformer: Rethinking spatial shuffle for vision transformer. *arXiv preprint arXiv:210603650*, .
- Ioffe S, Szegedy C, 2015. Batch normalization: Accelerating deep network training by reducing internal covariate shift. International conference on machine learning, p.448-456.
- Kingma DP, Ba J, 2014. Adam: A method for stochastic optimization. *arXiv preprint arXiv:1412.6980*, .
- Kirillov A, Girshick R, He K, et al., 2019a. Panoptic feature pyramid networks. CVPR, p.6399-6408.
- Kirillov A, Girshick R, He K, et al., 2019b. Panoptic feature pyramid networks. Proceedings of the IEEE/CVF Conference on Computer Vision and Pattern Recognition, p.6399-6408.
- Krizhevsky A, Sutskever I, Hinton GE, 2012. Imagenet classification with deep convolutional neural networks. *Advances in neural information processing systems*, 25:1097-1105.
- Lee H, Kim HE, Nam H, 2019. Srm: A style-based recalibration module for convolutional neural networks. Proceedings of the IEEE/CVF International Conference on Computer Vision, p.1854-1862.
- Li D, Hu J, Wang C, et al., 2021. Involution: Inverting the inheritance of convolution for visual recognition. Proceedings of the IEEE/CVF Conference on Computer Vision and Pattern Recognition, p.12321-12330.
- Li J, Wang J, Tian Q, et al., 2019a. Global-local temporal representations for video person re-identification. Proceedings of the IEEE/CVF international conference on computer vision, p.3958-3967.
- Li X, Wang W, Hu X, et al., 2019b. Selective kernel networks. Proceedings of the IEEE/CVF conference on computer vision and pattern recognition, p.510-519.
- Lin TY, Maire M, Belongie S, et al., 2014a. Microsoft coco: Common objects in context. European conference on computer vision, p.740-755.

- Lin TY, Maire M, Belongie S, et al., 2014b. Microsoft coco: Common objects in context. *ECCV*, p.740-755.
- Lin TY, Goyal P, Girshick R, et al., 2017a. Focal loss for dense object detection. *ICCV*, p.2980-2988.
- Lin TY, Goyal P, Girshick R, et al., 2017b. Focal loss for dense object detection. *Proceedings of the IEEE international conference on computer vision*, p.2980-2988.
- Liu H, Simonyan K, Yang Y, 2018. Darts: Differentiable architecture search. *arXiv preprint arXiv:180609055*, .
- Liu H, Dai Z, So D, et al., 2021a. Pay attention to MLPs. *NeurIPS*.
- Liu Z, Lin Y, Cao Y, et al., 2021b. Swin transformer: Hierarchical vision transformer using shifted windows. *Proceedings of the IEEE/CVF International Conference on Computer Vision (ICCV)*, p.10012-10022.
- Liu Z, Lin Y, Cao Y, et al., 2021c. Swin transformer: Hierarchical vision transformer using shifted windows. *ICCV*.
- Liu Z, Wang L, Wu W, et al., 2021d. Tam: Temporal adaptive module for video recognition. *Proceedings of the IEEE/CVF International Conference on Computer Vision*, p.13708-13718.
- Liu Z, Mao H, Wu CY, et al., 2022. A convnet for the 2020s. *arXiv preprint arXiv:220103545*, .
- Loshchilov I, Hutter F, 2016. Sgdr: Stochastic gradient descent with warm restarts. *arXiv preprint arXiv:160803983*, .
- Loshchilov I, Hutter F, 2018. Decoupled weight decay regularization. *International Conference on Learning Representations*.
- Pan Z, Zhuang B, He H, et al., 2022. Less is more: Pay less attention in vision transformers. *Proceedings of the AAAI Conference on Artificial Intelligence*, 36(2):2035-2043.
- Park N, Kim S, 2022. How do vision transformers work? *arXiv preprint arXiv:220206709*, .
- Radosavovic I, Kosaraju RP, Girshick R, et al., 2020. Designing network design spaces. *Proceedings of the IEEE/CVF conference on computer vision and pattern recognition*, p.10428-10436.
- Rao Y, Zhao W, Zhu Z, et al., 2021. Global filter networks for image classification. *Advances in Neural Information Processing Systems*, 34:980-993.
- Real E, Aggarwal A, Huang Y, et al., 2019. Regularized evolution for image classifier architecture search. *Proceedings of the aaai conference on artificial intelligence*, 33(01):4780-4789.
- Selvaraju RR, Cogswell M, Das A, et al., 2017. Grad-cam: Visual explanations from deep networks via gradient-based localization. *ICCV*, p.618-626.
- Simonyan K, Zisserman A, 2015. Very deep convolutional networks for large-scale image recognition. *3rd International Conference on Learning Representations, ICLR 2015, San Diego, CA, USA, May 7-9, 2015, Conference Track Proceedings*, <http://arxiv.org/abs/1409.1556>
- Szegedy C, Vanhoucke V, Ioffe S, et al., 2016. Rethinking the inception architecture for computer vision. *Proceedings of the IEEE conference on computer vision and pattern recognition*, p.2818-2826.
- Tan M, Le Q, 2019a. Efficientnet: Rethinking model scaling for convolutional neural networks. *International conference on machine learning*, p.6105-6114.
- Tan M, Le QV, 2019b. Mixconv: Mixed depthwise convolutional kernels. *arXiv preprint arXiv:190709595*, .
- Touvron H, Bojanowski P, Caron M, et al., 2021a. Resmlp: Feedforward networks for image classification with data-efficient training. *arXiv preprint arXiv:210503404*, .
- Touvron H, Cord M, Douze M, et al., 2021b. Training data-efficient image transformers & distillation through attention. *International Conference on Machine Learning*, p.10347-10357.
- Vaswani A, Shazeer N, Parmar N, et al., 2017. Attention is all you need. *Advances in neural information processing systems*, p.5998-6008.
- Vaswani A, Ramachandran P, Srinivas A, et al., 2021. Scaling local self-attention for parameter efficient visual backbones. *Proceedings of the IEEE/CVF Conference on Computer Vision and Pattern Recognition*, p.12894-12904.
- Wang W, Xie E, Li X, et al., 2021a. Pvtv2: Improved baselines with pyramid vision transformer. *arXiv preprint arXiv:210613797*, .
- Wang W, Xie E, Li X, et al., 2021b. Pyramid vision transformer: A versatile backbone for dense prediction without convolutions. *Proceedings of the IEEE/CVF International Conference on Computer Vision (ICCV)*, p.568-578.
- Wang W, Xie E, Li X, et al., 2021c. Pyramid vision transformer: A versatile backbone for dense prediction without convolutions. *ICCV*.
- Wang X, Girshick R, Gupta A, et al., 2018. Non-local neural networks. *CVPR*, p.7794-7803.
- Wu B, Dai X, Zhang P, et al., 2019. Fbnet: Hardware-aware efficient convnet design via differentiable neural architecture search. *Proceedings of the IEEE/CVF Conference on Computer Vision and Pattern Recognition*, p.10734-10742.
- Wu YH, Liu Y, Xu J, et al., 2021. Mobilesal: Extremely efficient rgb-d salient object detection. *IEEE Transactions on Pattern Analysis and Machine Intelligence*, .
- Xiao T, Liu Y, Zhou B, et al., 2018. Unified perceptual parsing for scene understanding. *ECCV*, p.418-434.
- Xie S, Girshick R, Dollár P, et al., 2017. Aggregated residual transformations for deep neural networks. *Proceedings of the IEEE conference on computer vision and pattern recognition*, p.1492-1500.
- Yang B, Bender G, Le QV, et al., 2019. Condconv: Conditionally parameterized convolutions for efficient inference. *Advances in Neural Information Processing Systems*, 32.
- Yang J, Li C, Zhang P, et al., 2021. Focal self-attention for local-global interactions in vision transformers. *arXiv preprint arXiv:210700641*, .
- Yu M, Luo M, Zhou P, et al., 2021. Metaformer is actually what you need for vision. *arXiv preprint arXiv:211111418*, .
- Yuan L, Chen Y, Wang T, et al., 2021. Tokens-to-token vit: Training vision transformers from scratch on imagenet. *ICCV*, p.558-567.

- Yun S, Han D, Oh SJ, et al., 2019. Cutmix: Regularization strategy to train strong classifiers with localizable features. *ICCV*, p.6023-6032.
- Zhang H, Cisse M, Dauphin YN, et al., 2018. mixup: Beyond empirical risk minimization. *International Conference on Learning Representations*.
- Zhao H, Zhang Y, Liu S, et al., 2018. Psanet: Point-wise spatial attention network for scene parsing. *Proceedings of the European conference on computer vision (ECCV)*, p.267-283.
- Zhou B, Zhao H, Puig X, et al., 2017. Scene parsing through ade20k dataset. *Proceedings of the IEEE conference on computer vision and pattern recognition*, p.633-641.
- Zhou B, Zhao H, Puig X, et al., 2019. Semantic understanding of scenes through the ade20k dataset. *IJCV*, 127(3):302-321.